

# Elastic and inelastic SU(3)-breaking final-state interactions in $B$ decays to pseudoscalar mesons

P. Żenczykowski\* and P. Łach

*Dept. of Theoretical Physics, Institute of Nuclear Physics  
Polish Academy of Sciences  
Radzikowskiego 152, 31-342 Kraków, Poland*

February 1, 2008

## Abstract

We discuss all contributions from the Zweig-rule-satisfying SU(3)-breaking final state interactions (FSIs) in the  $B \rightarrow PP$  decays (neglecting charmed intermediate states), where  $PP = \pi\pi$ ,  $\pi K$ ,  $K\bar{K}$ ,  $\pi\eta(\eta')$ , and  $K\eta(\eta')$ . First, effects of SU(3) breaking in rescattering through Pomeron exchange are studied. Then, after making a plausible assumption concerning the pattern of SU(3) breaking in non-Pomeron FSIs, we give general formulas for how the latter modify short-distance (SD) amplitudes. In the SU(3) limit, these formulas depend on three effective parameters characterizing the strength of all non-Pomeron rescattering effects. We point out that the experimental bounds on the  $B \rightarrow K^+K^-$  branching ratio may limit the value of only one of these FSI parameters. Thus, the smallness of the  $B \rightarrow K^+K^-$  decay rate does not imply negligible rescattering effects in other decays. Assuming a vanishing value of this parameter, we perform various fits to the available  $B \rightarrow PP$  branching ratios. The fits determine the quark-diagram SD amplitudes, the two remaining FSI parameters and the weak angle  $\gamma$ . While the set of all  $B \rightarrow PP$  branching ratios is well described with  $\gamma$  around its expected Standard Model (SM) value, the fits permit other values of  $\gamma$  as well. For a couple of such good fits, we predict asymmetries for the  $B \rightarrow K\pi$ ,  $\pi^+\eta(\eta')$ ,  $K^+\eta(\eta')$  decays as well as the values of the CP-violating parameters  $S_{\pi\pi}$  and  $C_{\pi\pi}$  for the time-dependent rate of  $B^0(t) \rightarrow \pi^+\pi^-$ . Apart from a problem with the recent  $B^+ \rightarrow \pi^+\eta$  asymmetry measurement, comparison with the data seems to favour the values of  $\gamma$  in accordance with SM expectations.

PACS numbers: 13.25.Hw, 11.30.Hv, 12.15.Hh, 11.80.Gw

\* E-mail: zenczyko@iblis.ifj.edu.pl

# 1 Introduction

The majority of the analyses of CP-violating effects in  $B$  decays assume that the relevant amplitudes are given by short-distance (SD) expressions only. In particular, for  $B$  decays into two pseudoscalar mesons ( $B \rightarrow PP$ ), any possible final state interactions (FSIs) are usually completely neglected. It is very difficult to assess if this neglect is justified or not. Some authors have argued that such effects should be negligible [1, 2] since the  $B$  mass is already quite large. In other papers it is stressed that the FSIs should be important and that any reliable analyses of  $B$  decays must take these interactions into account [3, 4, 5, 6, 7]. It has been suspected that the inelastic FSIs are particularly important [3, 6]. Unfortunately, with our insufficient knowledge of the  $PP$  interactions at  $5.2\text{ GeV}$ , there is virtually no hope that the relevant rescattering effects may be calculated reliably.

In order to overcome this obstacle, in a recent paper [8] we analysed an SU(3)-symmetric approach with the built-in Zweig rule, in which our ignorance as to the size of inelastic rescattering was reduced to a set of only three *effective* (complex) parameters jointly describing all inelastic final state interaction (IFSI) effects. It was shown that the SU(3)-symmetric rescattering leads to a simple redefinition of quark-diagram amplitudes, thus permitting the use of a diagram description in which, however, weak phases may enter in a modified way. Furthermore, a simple estimate was made as to the size of error which could be committed while extracting the value of the unitarity-triangle angle  $\gamma$  when such modifications are not taken into account.

In the present paper, we extend the general scheme of ref.[8] and introduce SU(3) breaking both in the elastic and in the inelastic final state interactions. The introduction of SU(3) breaking makes it reasonable to attempt a detailed description of the data. When doing so, we take into account all short-distance amplitudes usually considered as the dominant ones (Section 2), and make certain assumptions as to the form of FSIs and SU(3) breaking (Sections 3 and 4). In Section 4 we also discuss at some length the point that estimating the size of all rescattering effects on the basis of the  $B \rightarrow K\bar{K}$  data is significantly more difficult than usually acknowledged. Then, in Section 5, we perform fits to the experimental branching ratios of the  $B \rightarrow PP$  decays, and discuss their implications. A brief summary appears in Section 6.

## 2 Short-distance amplitudes

Short-distance amplitudes may lead not only to the  $PP$  states but also to the general  $M_1M_2$  states, with  $M_i$  representing various heavy mesons. Consequently, the  $PP$  pair observed in  $B$  decay may be produced in three ways: it may not participate in any rescattering after being produced in a SD process, it may undergo elastic rescattering, and, finally, it may result from inelastic rescattering of  $M_1M_2$  into  $PP$ . As discussed in [8], with the help of the unitarity condition, contributions from other inelastic intermediate states (such as many-body states  $M_1M_2\dots M_n$ ) may be always incorporated into the contribution from  $M_1M_2$ .

All SD amplitudes  $B \rightarrow M_1M_2$  may be classified in the same way as standard SD amplitudes  $B \rightarrow PP$ , ie.  $T, T'$  (tree),  $C, C'$  (colour suppressed),  $P, P'$  (penguin),  $E, E'$  (exchange),  $A, A'$  (annihilation),  $PA, PA'$  (penguin annihilation),  $S, S'$  (singlet penguin),  $SS, SS'$  (double singlet penguin). As usual, we denote strangeness-conserving  $\Delta S = 0$  (strangeness-violating  $|\Delta S| = 1$ ) processes by unprimed (primed) amplitudes respectively. Electroweak penguin contributions may be included via the replacements:  $T \rightarrow T + P_{EW}^c$ ,  $P \rightarrow P - P_{EW}^c/3$ ,  $C \rightarrow C + P_{EW}$ ,  $S \rightarrow S - P_{EW}/3$  [9] (with analogous expressions for the primed amplitudes).

The essential assumption of refs.[10, 8] is that the tree, penguin, etc. amplitudes for the production of various  $M_1M_2$  states are *proportional* to the corresponding amplitudes for the production of the  $PP$  pair. One may argue that the relevant coefficients of proportionality are approximately independent of the diagram type (tree, penguin, etc.) considered. The common remaining single coefficient of proportionality may be absorbed into the rescattering amplitudes  $M_1M_2 \rightarrow PP$ , for which the Zweig-rule is assumed. Finally, the sum over all intermediate states  $M_1M_2$  may be performed leading to the appearance of only three effective complex parameters representing the relevant sums and corresponding to the presence of three Zweig-rule satisfying SU(3)-symmetric forms for  $M_1M_2 \rightarrow PP$  (for more details, see [10, 8]).

As a result of these simplifications, all contributions from various short-distance  $B \rightarrow M_1M_2$  amplitudes get expressed in terms of relevant standard  $B \rightarrow PP$  short-distance amplitudes. Our whole approach to inelastic rescattering depends therefore on standard  $T, P, \dots P', T', \dots$  etc. amplitudes (with appropriate weak phases) and on parameters effectively describing the rescattering. In order to simplify the discussion and study the effect of FSIs only, we assume that the strong SD phases are negligible. (In ref.[1] these phases were estimated to be of the order of  $10^\circ$ , while in ref. [11] it is argued that the FSI-uncorrected "bare" amplitudes do not contain any strong phases - see the comment after Eq.(16) therein). This assumption may be relaxed

in future.

Some of the SD quark-diagram amplitudes are related. In an approach in which FSIs break SU(3), one should incorporate SU(3) breaking into the SD relationships as well. Therefore, we assume that the tree SD amplitudes satisfy the following relation [12]:

$$T' = \frac{V_{us}}{V_{ud}} \frac{f_K}{f_\pi} T \approx 0.276 T \quad (1)$$

Both tree amplitudes have the same (weak) phase:  $T/|T| = T'/|T'| = e^{i\gamma}$ .

The penguin SD amplitudes are dominated by the  $t$  quark, so that the weak phase factor is  $e^{-i\beta}$  for  $P$  and  $\pm 1$  for  $P'$  (ie.  $P' = \pm |P'|$ ). We use the estimate [12]

$$P = -e^{-i\beta} \left| \frac{V_{td}}{V_{ts}} \right| P' \approx -0.176 e^{-i\beta} P'. \quad (2)$$

In the fits of Section 5, we accept  $\beta = 24^\circ$ , which is in agreement with the world average [13]  $\sin 2\beta = 0.734 \pm 0.054$ . We accept (as it is usually done) that the value of the penguin SD amplitudes does not depend on the flavour of the quark-antiquark pair created to produce the  $M_1 M_2$  state. For example, standard SD contributions from penguin  $P$  in  $B_d^0 \rightarrow \pi^+ \pi^-$  (or  $\pi^0 \pi^0$ ), and in  $B^+ \rightarrow K^+ \bar{K}^0$  are given by SU(3) considerations only, despite the fact that in these two processes the produced quark-antiquark pairs are of different flavours.

We accept the relations between the tree and the colour-suppressed amplitudes given by the SD estimates:

$$C = \xi T \quad (3)$$

and

$$C' = T'(\xi - (1 + \xi)\delta_{EW}e^{-i\gamma}) \quad (4)$$

where we take  $\xi = \frac{C_1 + \zeta C_2}{C_2 + \zeta C_1} \approx 0.17$ , assuming  $\zeta \approx 0.42$ , ie. midway between  $1/N_c$  and the value of 0.5 suggested by experiment, and using  $C_1 \approx -0.31$  and  $C_2 \approx 1.14$  [14]. The contribution from the electroweak penguin  $P'_{EW}$  has been included in Eq.(4), with  $\delta_{EW} \approx +0.65$  [15] (other electroweak penguins are neglected).

The last independent SD amplitude considered here is the singlet penguin amplitude  $S'$ , whose weak phase is 0 (data requires that this amplitude be sizable [16, 12]). Thus, the SD amplitudes and our whole approach depend on four SD parameters:  $|T|$ ,  $P'$ ,  $S'$ , and the weak phase  $\gamma$ . The remaining SD amplitudes ( $E, E', S, PA, \dots$ ) are assumed to be negligible.

### 3 SU(3)-breaking in Pomeron-exchange-induced rescattering

If we gather all SD amplitudes  $B \rightarrow PP$  (as well as those of  $B \rightarrow M_1 M_2$ ) into vector  $\mathbf{w}$ , and accept that FSIs cannot modify the probabilities of the original SD weak decays, it follows that vector  $\mathbf{W}$  representing the set of all FSI-corrected amplitudes is related to  $\mathbf{w}$  through [6, 10]:

$$\mathbf{W} = \mathbf{S}^{1/2} \mathbf{w}, \quad (5)$$

(in the one-channel case, Eq.(5) reduces to the Watson's theorem [17]).

Let us consider now elastic  $PP$  rescattering only (ie. with  $\mathbf{w}$  restricted to its part corresponding to  $B \rightarrow PP$  processes, and similarly for  $\mathbf{W}$ ). For high energies this rescattering is approximately independent of energy. We shall use Regge terminology and call this energy-independent term a Pomeron-induced contribution. Since Pomeron exchange is known to be substantial, the  $B \rightarrow PP$  amplitudes at  $s = m_B^2$  should be corrected for Pomeron-induced rescattering. Treating Pomeron-induced FSIs as a small correction to the SD expressions for  $B \rightarrow PP$  amplitudes corresponds to expanding  $\mathbf{S}^{1/2} \equiv (\mathbf{1} + i\mathbf{T})^{1/2} = (\mathbf{1} + 2i\mathbf{A})^{1/2} = \mathbf{1} + i\mathbf{A} + \dots$  and keeping terms linear in  $\mathbf{A}$  only. Thus, one gets [6]:

$$\mathbf{W} \approx (\mathbf{1} + i\mathbf{A})\mathbf{w} \quad (6)$$

Because the amplitudes for Pomeron exchange are predominantly imaginary, we have

$$\mathbf{A} = i\mathbf{a} \quad (7)$$

with real  $\mathbf{a}$ . In the SU(3)-symmetric world, all elements of  $\mathbf{a}$  are identical, and their common value is  $a \approx 0.16$  (cf [3] and Eqs.(10,17) in [6]). Consequently, Pomeron-induced rescattering rescales all SD amplitudes in the same way:

$$\mathbf{W} = (1 - a)\mathbf{w}. \quad (8)$$

It is only when SU(3) is broken that the rescaling is different for different decay channels, and deviations from the standard SD form could be observed in principle.

When SU(3) is broken, the values of  $a$  differ for different final channels  $P_1 P_2$ . In a simple model for Pomeron used in [3, 18], they are given by

$$a(P_1 P_2) = \frac{1}{16\pi} \frac{\beta_{P_1} \beta_{P_2}}{b_{P_1} + b_{P_2}} \quad (9)$$

with the values of  $\beta_\pi$ ,  $\beta_K$  (meson-Pomeron couplings) and  $b_\pi$ ,  $b_K$  (slope coefficients for the relevant couplings) extracted from data on  $\pi p$  and  $Kp$  scattering. In the following we will use the averages of values given in [3, 18], ie.:

$$\begin{aligned}\beta_\pi &= 3.47 \sqrt{\text{mb}} \\ \beta_K &= 2.78 \sqrt{\text{mb}} \\ b_\pi &= 1.93 \text{ GeV}^{-2} \\ b_K &= 0.9 \text{ GeV}^{-2}\end{aligned}\tag{10}$$

In order to estimate  $\beta_\eta$ ,  $\beta_{\eta'}$  and  $b_\eta$ ,  $b_{\eta'}$ , we assume perfect mixing for  $\eta, \eta'$  (ie.  $\eta = (u\bar{u} + d\bar{d} - s\bar{s})/\sqrt{3}$ , and  $\eta' = (u\bar{u} + d\bar{d} + 2s\bar{s})/\sqrt{6}$ ) corresponding to the octet-singlet mixing angle of  $\theta = -19.5^\circ$ , (see eg. [19, 20, 21, 16]; for a different approach to  $\eta - \eta'$  mixing in  $B \rightarrow K\eta^{(\prime)}$  decays see [22]), and derive [18]:

$$\begin{aligned}\beta_\eta &= (\beta_\pi + 2\beta_K)/3 \approx 3.01 \sqrt{\text{mb}} \\ \beta_{\eta'} &= (-\beta_\pi + 4\beta_K)/3 \approx 2.55 \sqrt{\text{mb}} \\ b_\eta &= (b_\pi + 2b_K)/3 \approx 1.24 \text{ GeV}^{-2} \\ b_{\eta'} &= (-b_\pi + 4b_K)/3 \approx 0.56 \text{ GeV}^{-2}\end{aligned}\tag{11}$$

Note that for the  $K\eta'$  channel the denominator in Eq.(9) is particularly small. In this channel the Pomeron-exchange-induced correction is therefore relatively large which may possibly affect the extraction of the short-distance  $S'$  amplitude from the data.

The resulting pattern of SD amplitudes corrected for Pomeron-induced rescattering differs from standard SD expressions by departures from SU(3) only. Consequently, we introduce SU(3)-symmetric rescaled amplitudes  $\bar{T}$ ,  $\bar{T}'$ ,  $\bar{P}$ ,  $\bar{P}'$ , ..etc., defined as

$$\begin{aligned}\bar{T}^{(\prime)} &= T^{(\prime)}(1 - a(\pi\pi)) \\ \bar{P}^{(\prime)} &= P^{(\prime)}(1 - a(\pi\pi)) \\ &\dots\end{aligned}\tag{12}$$

and the SU(3)-breaking corrections  $K(P_1 P_2) = (a(\pi\pi) - a(P_1 P_2))/(1 - a(\pi\pi))$ . The complete set of SD amplitudes corrected for SU(3)-breaking Pomeron-exchange-induced rescattering is gathered in Table 1.

Table 1: SD amplitudes for decays  $B^+, B_d^0 \rightarrow P_1 P_2$  corrected for SU(3)-breaking Pomeron-exchange-induced rescattering

Decay	rescaled and corrected SD
$B^+ \rightarrow \pi^+ \pi^0$	$-\frac{1}{\sqrt{2}}(\bar{T} + \bar{C})$
$K^+ \bar{K}^0$	$-\bar{P}(1 + K(KK))$
$\pi^+ \eta$	$-\frac{1}{\sqrt{3}}(\bar{T} + \bar{C} + 2\bar{P})(1 + K(\pi\eta))$
$\pi^+ \eta'$	$-\frac{1}{\sqrt{6}}(\bar{T} + \bar{C} + 2\bar{P})(1 + K(\pi\eta'))$
$B_d^0 \rightarrow \pi^+ \pi^-$	$-(\bar{T} + \bar{P})$
$\pi^0 \pi^0$	$-\frac{1}{\sqrt{2}}(\bar{C} - \bar{P})$
$K^+ K^-$	0
$K^0 \bar{K}^0$	$-\bar{P}(1 + K(KK))$
$B^+ \rightarrow \pi^+ K^0$	$-\bar{P}'(1 + K(\pi K))$
$\pi^0 K^+$	$\frac{1}{\sqrt{2}}(\bar{T}' + \bar{C}' + \bar{P}')(1 + K(\pi K))$
$\eta K^+$	$\frac{1}{\sqrt{3}}(\bar{T}' + \bar{C}' + \bar{S}')(1 + K(\eta K))$
$\eta' K^+$	$\frac{1}{\sqrt{6}}(\bar{T}' + \bar{C}' + 3\bar{P}' + 4\bar{S}')(1 + K(\eta' K))$
$B_d^0 \rightarrow \pi^- K^+$	$(\bar{T}' + \bar{P}')(1 + K(\pi K))$
$\pi^0 K^0$	$\frac{1}{\sqrt{2}}(\bar{C}' - \bar{P}')(1 + K(\pi K))$
$\eta K^0$	$\frac{1}{\sqrt{3}}(\bar{C}' + \bar{S}')(1 + K(\eta K))$
$\eta' K^0$	$\frac{1}{\sqrt{6}}(\bar{C}' + 3\bar{P}' + 4\bar{S}')(1 + K(\eta' K))$

## 4 Inelastic SU(3)-breaking FSI with Zweig rule

Analysis of inelastic SU(3)-breaking effects follows the approach of [8]. As in ref. [8], in the present paper we do not consider contributions from intermediate charmed states (thus neglecting the long-distance "charming penguins"). Since they may be important [23, 24, 25, 26, 11], their analysis merits further work. The most general Zweig-rule-satisfying rescattering  $M_1 M_2 \rightarrow P_1 P_2$  is described by two types of connected diagrams: the "uncrossed" diagrams of Fig.1(u), and the "crossed" diagrams of Fig.1(c). By virtue of Bose statistics, the final  $P_1 P_2$  pair must be in an overall symmetric state. Our definition of inelastic rescattering includes a non-Pomeron contribution from  $P_1 P_2 \rightarrow P_1 P_2$  transitions, which - together with the Pomeron-exchange-induced part of these transitions - are usually classified as elastic.

## 4.1 SU(3)-invariant rescattering amplitudes

In the SU(3) case, the requirement of Bose statistics for  $P_1 P_2$  means that there are two types of uncrossed  $M_1 M_2 \rightarrow P_1 P_2$  amplitudes, ie. (using a particle symbol for the corresponding SU(3) matrix):

$$\text{Tr}(\{M_1^\dagger, M_2^\dagger\}\{P_1, P_2\}) u_+ \quad (13)$$

and

$$\text{Tr}([M_1^\dagger, M_2^\dagger]\{P_1, P_2\}) u_- \quad (14)$$

where the requirement in question is reflected by the presence of the anticommutator  $\{P_1, P_2\}$  of meson matrices, and  $u_\pm$  denote the strength of rescattering amplitudes. Eqs.(13,14) incorporate nonet symmetry for both intermediate and final mesons. As explained in [8], invariance of strong interactions under charge conjugation demands that mesons  $M_1$  and  $M_2$  belong to multiplets of the same (opposite) C-parities for the first (second) amplitude above.

For the crossed diagrams, the requirement of  $P_1 \rightleftharpoons P_2$  symmetry admits one combination only [8]:

$$\text{Tr}(M_1^\dagger P_1 M_2^\dagger P_2 + M_1^\dagger P_2 M_2^\dagger P_1) c \quad (15)$$

where  $c$  denotes amplitude strength. This combination is symmetric under  $M_1 \rightleftharpoons M_2$  as well. Consequently, it is charge-conjugation invariant if  $M_1$  and  $M_2$  have C-parities of the same sign.

## 4.2 Modifications due to SU(3) breaking

We will incorporate SU(3) breaking into the FSI amplitudes of Eqs.(13, 14, 15) in the simplest possible way. First let us consider  $u$ -type diagrams (Fig.1(u)). In these diagrams one quark (or antiquark) from meson  $M_1$  ends up in the final pseudoscalar meson, while the other one annihilates an antiquark (quark) from meson  $M_2$ . It is well known that such quark-antiquark annihilations are suppressed when the relevant  $q\bar{q}$  pair has high energy, and that they are suppressed even more strongly for the  $s\bar{s}$  pair. In the Regge language, the first statement corresponds to meson exchanges being suppressed at high energies, the latter - to the fact that intercepts of Regge trajectories for mesons containing strange quarks lie below those for mesons composed of  $u, d, \bar{u}, \bar{d}$  only. The additional suppression of  $s\bar{s}$  annihilation with respect to that of  $u\bar{u}$  (or  $d\bar{d}$ ) depends on the energy of the  $q\bar{q}$  pair. Since we want to analyse the main effect of SU(3) breaking only, we assume that an exchange of



a strange (anti)quark between mesons  $M_1$  and  $M_2$  (or between  $P_1$  and  $P_2$ ) is suppressed by the same factor ( $\epsilon$ ) for all intermediate states. On the other hand, the amplitudes for the uncrossed diagrams in which strange (anti)quarks from mesons  $M_1$  end up in final pseudoscalar mesons (ie. are not annihilated) are not suppressed by SU(3)-breaking effects.

The relevant  $u$ -type amplitudes may be then calculated from the appropriate generalizations of Eqs.(13,14). For the contribution from mesons  $M_1$  and  $M_2$  of the same charge-conjugation parities ( $C(M_1)C(M_2) = +1$ ) we have, for example:

$$\begin{aligned} & \frac{1}{2}\text{Tr}((M_1^\dagger I_\epsilon M_2^\dagger + M_2^\dagger I_\epsilon M_1^\dagger)(P_1 I_\epsilon P_2 + P_2 I_\epsilon P_1)) u_+ \\ & + \frac{1}{2}\text{Tr}((M_1^{\dagger T} I_\epsilon M_2^{\dagger T} + M_2^{\dagger T} I_\epsilon M_1^{\dagger T})(P_1^T I_\epsilon P_2^T + P_2^T I_\epsilon P_1^T)) u_+ \end{aligned} \quad (16)$$

where

$$I_\epsilon = \begin{bmatrix} 1 & 0 & 0 \\ 0 & 1 & 0 \\ 0 & 0 & \epsilon \end{bmatrix}. \quad (17)$$

In Eq.(16) we divided the whole contribution into two parts, depending on whether it is the strange quark or antiquark from (say)  $M_1$  which is annihilated. Contributions from the  $C(M_1)C(M_2) = -1$  states may be calculated in a similar way (one has to remember that the negative sign between  $M_1 I_\epsilon M_2$  and  $M_2 I_\epsilon M_1$  is cancelled by the negative sign in the (antisymmetric) wave function of  $C(M_1)C(M_2) = -1$  two-meson states).

Since SU(3) is to be broken, the choice of definite SU(3) representations for the intermediate  $M_1 M_2$  states is not appropriate. Admitting the linear combinations of  $\mathbf{27}$ ,  $\mathbf{8_s}$ ,  $\mathbf{8_{\{81\}}}$ ,  $\mathbf{1_{\{88\}}}$ ,  $\mathbf{1_{\{11\}}}$ , and  $\mathbf{8_a}$  (considered in [8]) is not sufficient either, since for broken SU(3) the complete set of  $M_1 M_2$  intermediate states contains admixtures from other SU(3) representations. If all the  $C(M_1)C(M_2) = \pm 1$  intermediate states are to be taken into account properly, one may first list all states of definite charge, strangeness and isospin, and composed of two mesons of definite type, ie. with flavour quantum numbers of  $\pi K$  or  $\eta K$  or... . These states may be ordered (in the sense that  $\pi K$  is different from  $K\pi$ ) or, alternatively, their symmetric or antisymmetric combinations (under  $\pi \leftrightarrow K$  etc. interchanges) may be formed. Then, SD decay amplitudes into these states have to be evaluated. Finally, the sum over the contributions from all such states has to be carried out.

We have performed all the necessary calculations with the result that the sum over *all*  $C(M_1)C(M_2) = \pm 1$  intermediate states leads to the formulas given in the

second column of Table 2, where

$$\begin{aligned}\bar{u} &= u \frac{1}{1 - a(\pi\pi)} = \frac{u_+ + u_-}{2} \frac{1}{1 - a(\pi\pi)} \\ \bar{d} &= d \frac{1}{1 - a(\pi\pi)} = (u_+ - u_-) \frac{1}{1 - a(\pi\pi)}\end{aligned}\quad (18)$$

and

$$\begin{aligned}\Delta &= ((2 + \epsilon)\bar{P} + \bar{T}) \bar{d} \\ \Delta' &= ((2 + \epsilon)\bar{P}' + \bar{T}' + \epsilon\bar{S}') \bar{d}.\end{aligned}\quad (19)$$

Thus, the inelastic corrections are given in terms of the products of the SD amplitudes and the FSI parameters (here:  $u, d$ ). For example, there may be a contribution proportional to  $Td$ . Since we finally express all formulas in terms of the amplitudes modified for Pomeron-induced rescattering (eg. in terms of  $\bar{T} = T(1 - a(\pi\pi))$  etc.), in Eq.(18) we introduced the rescaled FSI parameters  $\bar{u}$  and  $\bar{d}$  so that eg.  $Td = \bar{T}\bar{d}$ . For completeness, in Table 2 we give formulas for the  $B_s^0$  decays as well.

We incorporate SU(3) breaking into the  $c$ -type amplitudes in a completely analogous fashion. Namely, we assume that strange (anti)quark interchanges are suppressed by factor  $\epsilon$  (in general, this factor may be different from that used for  $u$ -type diagrams). The relevant  $c$ -type amplitudes may be then calculated from an appropriate generalization of Eq.(15). As pointed out in [8], charge conjugation invariance of strong interactions requires that only symmetric  $M_1 M_2$  states contribute. For broken SU(3), Eq.(15) is replaced by

$$\begin{aligned}& \frac{1}{2} \text{Tr}(M_1^\dagger I_\epsilon P_1 M_2^\dagger I_\epsilon P_2 + M_1^\dagger I_\epsilon P_2 M_2^\dagger I_\epsilon P_1) c \\ & + \frac{1}{2} \text{Tr}(M_1^{\dagger T} I_\epsilon P_1^T M_2^{\dagger T} I_\epsilon P_2^T + M_1^{\dagger T} I_\epsilon P_2^T M_2^{\dagger T} I_\epsilon P_1^T) c\end{aligned}\quad (20)$$

As in Eq.(16), we divided the whole contribution into two parts depending on whether it is the strange quark or antiquark from (say)  $M_1$  which is exchanged. Using the above expression and the expressions for the SD amplitudes, and summing over all the intermediate states, one obtains the corrections induced by the  $c$ -type IFSIs. They are listed in the third column of Table 2, where

$$\bar{c} = c/(1 - a(\pi\pi))\quad (21)$$

In the limit of  $\epsilon \rightarrow 1$ , all formulas of Table 2 reduce to those given in [8], while for  $\epsilon = 0$  SU(3) is maximally broken.

Table 2: Inelastic SU(3)-breaking rescattering contributions:  $\Delta \equiv ((2 + \epsilon)\bar{P} + \bar{T}) \bar{d}$ ;  $\Delta' \equiv ((2 + \epsilon)\bar{P}' + \bar{T}' + \epsilon\bar{S}') \bar{d}$

Decay	uncrossed FSI diagrams	crossed FSI diagrams
$B^+ \rightarrow \pi^+ \pi^0$	0	$-\frac{1}{\sqrt{2}} 2\bar{c}(\bar{T} + \bar{C})$
$K^+ \bar{K}^0$	$-\epsilon(\Delta + 2\bar{u}\bar{C})$	0
$\pi^+ \eta$	$-\frac{2}{\sqrt{3}}(\Delta + 2\bar{u}\bar{C})$	$-\frac{1}{\sqrt{3}} 2\bar{c}(\bar{T} + \bar{C} + \bar{P}(2 - \epsilon))$
$\pi^+ \eta'$	$-\frac{2}{\sqrt{6}}(\Delta + 2\bar{u}\bar{C})$	$-\frac{1}{\sqrt{6}} 2\bar{c}(\bar{T} + \bar{C} + 2\bar{P}(1 + \epsilon))$
$B_d^0 \rightarrow \pi^+ \pi^-$	$-(\Delta + 2\bar{u}(\bar{T} + 2\bar{P}))$	$-2\bar{c}\bar{C}$
$\pi^0 \pi^0$	$\frac{1}{\sqrt{2}}(\Delta + 2\bar{u}(\bar{T} + 2\bar{P}))$	$-\frac{1}{\sqrt{2}} 2\bar{c}\bar{T}$
$K^+ K^-$	$2\bar{u}(\epsilon\bar{T} + (1 + \epsilon)\bar{P})$	0
$K^0 \bar{K}^0$	$-\epsilon\Delta - 2\bar{u}(1 + \epsilon)\bar{P}$	0
$\pi^0 \eta$	$-\frac{2}{\sqrt{6}}(\Delta - 2\bar{u}\bar{T})$	$-\frac{2}{\sqrt{6}}(2 - \epsilon)\bar{c}\bar{P}$
$\pi^0 \eta'$	$-\frac{1}{\sqrt{3}}(\Delta - 2\bar{u}\bar{T})$	$-\frac{1+\epsilon}{\sqrt{3}} 2\bar{c}\bar{P}$
$B_s^0 \rightarrow \pi^+ K^-$	$-\Delta$	$-(1 + \epsilon)\bar{c}\bar{C}$
$\pi^0 \bar{K}^0$	$\frac{1}{\sqrt{2}}\Delta$	$-\frac{1}{\sqrt{2}}(1 + \epsilon)\bar{c}\bar{T}$
$\eta \bar{K}^0$	$-\frac{1+\epsilon}{\sqrt{3}}\Delta$	$-\frac{1+\epsilon}{\sqrt{3}} \bar{c}((2 - \epsilon)\bar{P} + \bar{T})$
$\eta' \bar{K}^0$	$-\frac{1+2\epsilon}{\sqrt{6}}\Delta$	$-\frac{1+2\epsilon}{\sqrt{6}} \bar{c}(2(1 + \epsilon)\bar{P} + \bar{T})$
$B^+ \rightarrow \pi^+ K^0$	$-\Delta' - 2\bar{u}(\bar{C}' + \bar{S}')$	$-\bar{c}(1 + \epsilon)\bar{S}'$
$\pi^0 K^+$	$\frac{1}{\sqrt{2}}(\Delta' + 2\bar{u}(\bar{C}' + \bar{S}'))$	$\frac{1}{\sqrt{2}} \bar{c}(1 + \epsilon)(\bar{T}' + \bar{C}' + \bar{S}')$
$\eta K^+$	$\frac{1}{\sqrt{3}}(1 - \epsilon)(\Delta' + 2\bar{u}(\bar{C}' + \bar{S}'))$	$\frac{1}{\sqrt{3}} \bar{c}(1 + \epsilon)(\bar{T}' + \bar{C}' + \bar{P}'(2 - \epsilon) + \bar{S}'(1 - \epsilon))$
$\eta' K^+$	$\frac{1+2\epsilon}{\sqrt{6}}(\Delta' + 2\bar{u}(\bar{C}' + \bar{S}'))$	$\frac{1}{\sqrt{6}} \bar{c}(1 + \epsilon)(\bar{T}' + \bar{C}' + 2(1 + \epsilon)\bar{P}' + (1 + 2\epsilon)\bar{S}')$
$B_d^0 \rightarrow \pi^- K^+$	$\Delta' + 2\bar{u}\bar{S}'$	$\bar{c}(1 + \epsilon)(\bar{C}' + \bar{S}')$
$\pi^0 K^0$	$-\frac{1}{\sqrt{2}}(\Delta' + 2\bar{u}\bar{S}')$	$\frac{1}{\sqrt{2}} \bar{c}(1 + \epsilon)(\bar{T}' - \bar{S}')$
$\eta K^0$	$\frac{1}{\sqrt{3}}(1 - \epsilon)(\Delta' + 2\bar{u}\bar{S}')$	$\frac{1}{\sqrt{3}} \bar{c}(1 + \epsilon)(\bar{T}' + (2 - \epsilon)\bar{P}' + (1 - \epsilon)\bar{S}')$
$\eta' K^0$	$\frac{1+2\epsilon}{\sqrt{6}}(\Delta' + 2\bar{u}\bar{S}')$	$\frac{1}{\sqrt{6}} \bar{c}(1 + \epsilon)(\bar{T}' + 2(1 + \epsilon)\bar{P}' + (1 + 2\epsilon)\bar{S}')$
$B_s^0 \rightarrow \pi^+ \pi^-$	$-2\epsilon\bar{u}(2\bar{P}' + \bar{T}')$	0
$\pi^0 \pi^0$	$\sqrt{2}\epsilon\bar{u}(2\bar{P}' + \bar{T}')$	0
$K^+ K^-$	$\Delta' + 2\epsilon\bar{u}((1 + \epsilon)\bar{P}' + \epsilon\bar{T}' + \bar{S}')$	$2\epsilon\bar{c}(\bar{C}' + \bar{S}')$
$K^0 \bar{K}^0$	$-\Delta' - 2\epsilon\bar{u}((1 + \epsilon)\bar{P}' + \bar{S}')$	$-2\epsilon\bar{c}\bar{S}'$
$\pi^0 \eta$	$\frac{4}{\sqrt{6}}\epsilon\bar{u}\bar{T}'$	$-\frac{2}{\sqrt{6}}\epsilon\bar{c}\bar{T}'$
$\pi^0 \eta'$	$\frac{2}{\sqrt{3}}\epsilon\bar{u}\bar{T}'$	$\frac{2}{\sqrt{3}}\epsilon\bar{c}\bar{T}'$

### 4.3 Structure of full FSIs

For small inelastic final-state interactions, Eqs.(5,6) suggest the following approximation of all FSI effects:

$$\mathbf{W} \approx \mathbf{w} - \mathbf{a}\mathbf{w} + i\Delta\mathbf{W}_{\text{inel}} \quad (22)$$

where the three terms correspond to the contributions from the unmodified SD amplitudes, the Pomeron-exchange-induced corrections, and the inelastic FSI corrections (including the  $P_1P_2 \rightarrow P_1P_2$  elastic transitions not mediated by Pomeron) respectively. Here  $\Delta\mathbf{W}_{\text{inel}}$  (proportional to  $\sum_{M_1M_2} \mathbf{T}|M_1M_2\rangle\langle M_1M_2|\mathbf{w}$ ) is given by expressions for the inelastic FSIs gathered in Table 2. For negligible strong SD phases, it is the third term in Eq.(22) which allows the existence of direct CP violation effects. This term provides a specific prescription for how strong phases are generated by quark interchanges between outgoing mesons. In other words, the pattern of FSI phases in all  $B \rightarrow PP$  decays is governed by three (in general complex) parameters  $\bar{d}$ ,  $\bar{u}$ ,  $\bar{c}$  corresponding to different flavour-flow rescattering topologies and by the value of the SU(3)-breaking parameter(s)  $\epsilon$ .

### 4.4 Size of rescattering effects and $B \rightarrow KK$ decays

The Pomeron-induced FSIs and a contribution from non-Pomeron-mediated transitions  $P_1P_2 \rightarrow P_1P_2$  together comprise elastic rescattering. The non-Pomeron contributions to elastic transitions (eg. quark-line exchange diagrams for  $\pi^+\pi^- \rightarrow \pi^+\pi^-$ ) should be treated alongside symmetry-related contributions (ie.  $\pi^+\pi^- \rightarrow \pi^0\pi^0$  or  $\pi^+\pi^- \rightarrow K^+K^-$  etc.), as they all have common origin. For the SU(3) case all such "quasi-elastic"  $P'_1P'_2 \rightarrow P_1P_2$  transitions were estimated in the Regge approach [27]. The resulting differences between strong phases in the singlet, octet, and 27-plet  $PP$  channels (see also [18]) vanish at high energy, while at the  $B$ -meson mass they turn out to be nonnegligible yet small, of the order of  $10^\circ$ . Consequently, inclusion of full elastic FSIs should not lead to a significant change in the quality of data description (see also the fits of the next Section).

As for the inelastic rescattering, Table 2 provides the basis for the relevant discussion.

If FSIs satisfy SU(3) (ie. if  $\epsilon = 1$ ), all the  $\Delta$  and  $\Delta'$  terms in Table 2 may be absorbed into the new redefined penguins [8] (compare Eq.(22)):

$$\begin{aligned} \tilde{P} &= \bar{P} + i\Delta \\ \tilde{P}' &= \bar{P}' + i\Delta' \end{aligned} \quad (23)$$

With our assumptions of SU(3)-symmetric SD penguin amplitudes (cf. comment after Eq.(2)), such a redefinition is possible only if  $\epsilon = 1$  (compare the relevant  $\Delta$ -dependent corrections to  $B^+ \rightarrow K^+ \bar{K}^0$  and  $B_d^0 \rightarrow \pi^+ \pi^-$  in Table 2). As can be seen from the presence of the SD tree amplitudes in the redefined penguins in Eq.(23) (cf.  $\Delta = (3\bar{P} + \bar{T})\bar{d}$ ), parameter  $\bar{d}$  is related to the size of the long-distance ( $u$ -quark-loop) penguin. Formulas (23) indicate that contributions from penguin topologies with internal  $u$ -quark loops cannot lead to significant modification of total amplitudes - all such effects are consistently absorbed everywhere into new redefined penguins  $\tilde{P}$ ,  $\tilde{P}'$ . The only change is in the phase factors since  $\Delta$ 's include terms depending on  $\gamma$ . In general this leads to nonzero asymmetries, and should affect the determination of  $\gamma$ , as the (effective) amplitudes will now interfere in a different way.

In some papers it was argued that the  $B \rightarrow K^+ K^-$  decays could provide an estimate of the size of rescattering effects. Note, however, that this decay amplitude depends on  $u$  only. The  $B \rightarrow K^+ K^-$  branching ratio is independent of  $\bar{d}$  and  $\bar{c}$ , and, consequently, the size of long-distance penguins is not restricted by  $B \rightarrow K^+ K^-$ . This means that this branching ratio is not such a good place to estimate the "typical" size of FSI effects as it has been thought so far.

It is also sometimes said that the size of rescattering effects may be gleamed from the  $B^+ \rightarrow K^+ \bar{K}^0$  decay which is related to the  $B^+ \rightarrow \pi^+ K^0$  decay by an interchange of all down and strange quarks [29]. Here the standard argument assumes U-spin flavour symmetry of strong interactions. When SU(3) is broken, a look at Table 2 and Eqs. (19,23) shows that the conclusions from the comparison of  $B^+ \rightarrow K^+ \bar{K}^0$  and  $B^+ \rightarrow \pi^+ K^0$  decays *cannot* be obtained in such a simple way as originally thought. Namely, with the contribution from  $\bar{u}$ -generated FSI effects being bounded by the smallness of the  $B_d^0 \rightarrow K^+ K^-$  branching ratios, the FSI effects in  $B^+ \rightarrow K^+ \bar{K}^0$  are proportional to term  $\epsilon \Delta$ . However, on the basis of Regge ideas and our knowledge of high-energy multiparticle production processes in which  $K \bar{K}$  pairs are rarely produced, one expects that  $\epsilon$  is small. (The assumption of negligible  $\epsilon$  seems to be corroborated by the  $\epsilon$ -dependence of our fits below.) Consequently, the rescattering term in  $B^+ \rightarrow K^+ \bar{K}^0$  could be smaller by a factor of  $\epsilon$  from what is expected on the basis of U-spin symmetry with  $B^+ \rightarrow \pi^+ K^0$ . Therefore, despite the relative  $1/\lambda^2$  factor [29], the overall FSI effects in  $B^+ \rightarrow K^+ \bar{K}^0$  need not be much larger than those in  $B^+ \rightarrow \pi^+ K^0$ . Thus, from the smallness of FSI effects in  $B^+ \rightarrow K^+ \bar{K}^0$  one cannot infer that such effects are negligible elsewhere. In fact, a  $\Delta$ -induced term, such as that in  $B^+ \rightarrow K^+ \bar{K}^0$ , is present in all formulas in which the SD penguin  $P$  contributes. This leads (in the SU(3) limit) to the replacement of the original SD penguin amplitude  $\bar{P}$  by the effective penguin  $\tilde{P}$  given by Eq.

(23). It is only through a combined description of all the  $B \rightarrow PP$  branching ratios (and possibly asymmetries) such as these attempted in this paper (ie. not just of  $B^+ \rightarrow K^+\bar{K}^0$  and  $B^+ \rightarrow \pi^+K^0$  decays) that the effects induced by terms proportional to  $\Delta$  can be hopefully determined.

In order to study only the most important effects, we make now three assumptions for the fits of the next Section:

- 1) First, we put  $\epsilon = 0$  thus breaking SU(3) maximally.
- 2) Second, the present upper bound on the value of the  $B \rightarrow K^+K^-$  branching ratio ( $< 0.6 \cdot 10^{-6}$ ) limits the size of  $\bar{u}$  quite severely. Thus, we assume for simplicity that  $\bar{u} = 0$ .
- 3) Third, with no bounds set by  $B \rightarrow K^+K^-$  on  $\bar{d}$  and  $\bar{c}$  we must treat these parameters as free. However, while the value of  $\bar{d}$  could be complex, one expects that  $\bar{c}$  should be real (as required by the condition of no exotics in the  $s$ -channel - see Fig. 1(c); for the Regge model the corresponding expressions may be found in ref.[27]). Consequently, we will have three real parameters:  $\text{Re } \bar{d}$ ,  $\text{Im } \bar{d}$ ,  $\text{Re } \bar{c}$ .

With  $\epsilon$  fixed, our formulas depend on six real parameters:  $|\bar{T}|$ ,  $\bar{P}'$ ,  $\bar{S}'$ ,  $\text{Re } \bar{d}$ ,  $\text{Im } \bar{d}$ ,  $\text{Re } \bar{c}$  (in addition to weak phases). This may be compared to the approach of [28] which is less specific as to the origin of strong phases and involves seven independent hadronic parameters.

## 5 Fits

In order to estimate the effects which SU(3)-breaking rescattering may induce, we performed fits to the available branching ratios of B decays. We decided to compare the case with no FSIs (or with SU(3)-symmetric Pomeron-induced FSIs only) to the following two cases:

- (a) SU(3)-breaking Pomeron-exchange-induced FSIs only,
- (b) both Pomeron-exchange-induced and non-Pomeron SU(3)-breaking FSIs.

Since one of the objectives of this paper was to test the FSI effects, we assumed that the relative strong SD phases are negligible, ie. all direct CP violation effects involve only the long-distance strong phases generated by the FSI term  $i\Delta\mathbf{W}_{\text{inel}}$  in Eq.(22).

As the data constraining our fits we used only the branching ratios of the  $B \rightarrow PP$  decays (ie. we did not include the data on asymmetries). The first and the second column of Table 3 specify the decay channels  $i$  considered and the values

of the experimental branching ratios (and their errors) as used in our paper (from [12, 30, 31]). In the calculations themselves, the branching ratios were corrected for the deviation of the ratio of the  $\tau_{B^+}$  and  $\tau_{B^0}$  lifetimes from unity. The sum over all these decay channels  $i$  of the deviations between the experimental and theoretical branching ratios  $\mathbf{B}_i$  normalized to their experimental errors:

$$f(SD \text{ ampl}; FSI \text{ param.}) = \sum_i \frac{(\mathbf{B}_i(theor) - \mathbf{B}_i(exp))^2}{(\Delta \mathbf{B}_i(exp))^2}, \quad (24)$$

was subject to the minimization procedure (see eg.[1, 32]). Note that in our fits we used not only the  $B \rightarrow \pi\pi$  and  $B \rightarrow \pi K$  branching ratios (as in [1]), but also the remaining  $B \rightarrow PP$  branching ratios not considered elsewhere (in particular, those for  $B \rightarrow K\eta, K\eta'$ ). We performed several different fits, first keeping some of the arguments of  $f$  in Eq.(24) fixed, and then letting them free. The minimization procedure gave the best values of  $\bar{T}$ ,  $\bar{P}'$ , and  $\bar{S}'$  (for different values of weak phase  $\gamma$ ) as well as the values of the FSI parameters. The fits permitted predictions of CP asymmetries in  $B \rightarrow K\pi$ , the values of parameters  $S_{\pi\pi}$  and  $C_{\pi\pi}$  describing the behaviour of the time-dependent rates in  $B_d^0(t) \rightarrow \pi^+\pi^-$ , etc. Below we discuss our results in more detail.

## 5.1 Pomeron-induced rescattering

Consider first the situation with Pomeron-induced FSIs only, ie.  $\bar{d} = \bar{c} = \bar{u} = 0$ . Two cases differing with respect to the sign of (real)  $P'$  may be distinguished. A negative value of  $P'$  corresponds to vanishing differences of SD strong phases (eg.  $\delta_{P'}, \delta_{T'}$ ), while its positive value corresponds to this difference being  $180^\circ$ . Using  $P'$ ,  $|T|$ , and  $S'$  as free parameters, we minimized  $f$  for different values of  $\gamma$  for the no-FSI case (all  $a$ 's vanish), and for case (a) above. Dependence of the minimum value of  $f$  on the value of  $\gamma$  is shown in Fig.2. From Fig.2 (and Table 3) one can see that the introduction of SU(3)-breaking Pomeron-induced FSIs does not lead to a significant improvement in the description of data. Since non-Pomeron contributions to elastic rescattering cannot be large at  $B$  mass, this result is in contradiction with a recent paper [33] which claimed that data provide evidence for a large effect due to SU(3) breaking in elastic rescattering.

The preferred values of  $\gamma$  are in the range of around  $85^\circ < \gamma < 125^\circ$  ( $0^\circ < \gamma < 60^\circ$ ) for  $P' < 0$  ( $P' > 0$ ). The best fit is obtained for  $P' < 0$  with  $\gamma \approx 102^\circ$  (see Table 3), in agreement with earlier determinations preferring  $\gamma \gtrsim 90^\circ$  [1, 34, 35]. Such a large value of  $\gamma$  is in disagreement with the estimates in the Standard Model, which lead to  $\gamma_{SM} \approx 64.5^\circ \pm 7^\circ$  [34], or, more conservatively, to the region of  $50^\circ < \gamma < 80^\circ$

(see eg. [36, 37, 38]). The approach of ref.[28] permits slightly smaller values of  $\gamma$ , in the range of approximately  $75^\circ - 85^\circ$ , at the cost of introducing seven independent parameters in place of  $|T|$ ,  $P'$ , and  $S'$  (see also the next subsection). Table 3 shows that the inclusion of SU(3)-breaking Pomeron-induced FSIs enhances the value of the  $S'/P'$  ratio when extracting it from data.

## 5.2 Inelastic rescattering

Since even when  $\bar{u} = \epsilon = 0$  there are still three real FSI parameters ( $\text{Re } \bar{d}$ ,  $\text{Im } \bar{d}$ ,  $\text{Re } \bar{c}$ ), it is instructive to consider first the two limiting cases when 1)  $|\bar{d}| \ll |\bar{c}|$  and 2)  $|\bar{d}| \gg |\bar{c}|$ . In order to study these cases, we assume  $\bar{d} = 0$  or  $\bar{c} = 0$  respectively. The results of our fits for the  $P' > 0$  ( $P' < 0$ ) cases are shown in Fig.3a (Fig.3b). Solid (dashed) lines correspond to  $\bar{d} = 0$  ( $\bar{c} = 0$ ).

Clarification of how the curves in Fig.3 were obtained is in order. The approximation leading to Eq.(22) was based on the assumption that FSIs may be treated perturbatively. Consequently, the FSI parameters  $\bar{d}$ ,  $\bar{c}$  cannot be too large. Consider for example the  $dT$  correction to the penguin SD amplitude  $P$ . Since the ratio of  $|P|/|T|$  is expected to be around 0.3 (in our fits without FSIs we have  $= 0.73/2.58 = 0.28$ ), the admissible value of  $|\bar{d}|$  should be smaller than that number. Consequently, in the analysis leading to Fig.3 we limited the region of parameter values to  $|\text{Re } \bar{d}| < 0.25$ ,  $|\text{Im } \bar{d}| < 0.25$ . In order to give a feeling for the expected scale of FSI parameters, let us recall that the contribution to  $|u_+|$  arising from quasi-elastic non-Pomeron rescattering is fully calculable in the Regge model, and in ref.[8] it was estimated to be of the order of  $0.04 - 0.05$ . The value of  $|\bar{d}|$  of the order of 0.1 or 0.2 could therefore represent the sum of contributions from several intermediate channels while being still acceptable as corresponding to a perturbative realm.

When our restrictions on the allowed values of  $|\text{Re } \bar{d}|$ ,  $|\text{Im } \bar{d}|$  are relaxed, the global minima seen in Fig.3 are still present with the same values of  $f$ . For the  $P' > 0$  case (Fig.3a), the relevant curve lies only slightly below that shown. For the  $P' < 0$  case (Fig.3b), the minimum of the dashed curve on the right (at  $\gamma \approx 130^\circ$ ) becomes deeper with the value of  $f$  comparable to its value at  $\gamma \approx 60^\circ$ . However, the corresponding value of  $|\bar{d}|$  becomes significantly larger than 0.25. The fitted values of  $|\bar{c}|$  are of the order of 0.25 also when  $|\bar{c}|$  is not restricted. In the presented fits no restrictions on  $\bar{c}$  were imposed.

Comparison with Fig.2 shows that the minima of  $f$  treated as a function of  $\gamma$  are now deeper and significantly shifted when compared with the no-FSI case.



For the  $P' > 0$  case, we have: in the  $\bar{d} = 0$  case the minimum of  $f(\gamma)$  appears at  $\gamma \approx 50^\circ$  with a value of  $f$  at minimum being 12.2 and  $\bar{c} = -0.28$  (Fig.3a, solid line), while in the  $\bar{c} = 0$  case  $\gamma \approx 80^\circ$  is singled out with  $f = 13.3$  and  $\text{Re } \bar{d} = +0.25$ ,  $\text{Im } \bar{d} = -0.21$  (Fig.3a, dashed line). The reduced  $\chi_{red}^2 = f/(N - k)$ , with  $N = 15$  used as the number of data points, and  $k$  being the number of independent parameters, goes down from  $\chi_{red}^2$  around  $25/(15 - 4) \approx 2.2$  for the no-FSI case to  $\chi_{red}^2$  around  $1.2 - 1.4$  when FSI is taken into account.

For the  $P' < 0$  case, the minima of  $f(\gamma)$  are significantly deeper: in the  $\bar{d} = 0$  case there is a slight shift in  $\gamma$  (from around  $102^\circ$  to around  $90^\circ$ ) with the value of  $f(\gamma)$  at minimum being 8.84 and  $\bar{c} = 0.24$  (Fig.3b, solid line); in the  $\bar{c} = 0$  case the shift in  $\gamma$  is larger and a minimum appears at  $\gamma = 57^\circ$  with the value of  $f(\gamma)$  at minimum being 7.61 (Fig.3b, dashed line). In the latter case the fitted values of FSI parameters are

$$\text{Re } \bar{d} \approx -0.22 \quad (25)$$

$$\text{Im } \bar{d} \approx +0.21 \quad (26)$$

In both cases the value of  $\chi_{red}^2$  is about 0.9. The second minimum of the dashed line in Fig.3b at  $\gamma \approx 130^\circ$  corresponds to a different sign of  $\text{Re } \bar{d}$ . When the restriction on the size of  $|\bar{d}|$  is relaxed, this minimum becomes as deep as that at  $\gamma = 57^\circ$ . Then, however, the value of  $|\bar{d}|$  is much larger than 0.25. Since  $\chi_{red}^2$  is significantly smaller for  $P' < 0$ , we restrict further discussion to this case.

In Fig.4, relaxing for a moment the assumption  $\epsilon = 0$ , we show the  $\epsilon$ -dependence of the minimal values of  $f$  for  $P' < 0$  and for fixed values of  $\gamma$  in the two cases of  $\bar{d} = 0$  (Fig.4a) and  $\bar{c} = 0$  (Fig.4b). The region of small  $\epsilon$  seems to be preferred in both cases. In this analysis, as in that leading to Fig.3, the values of  $\bar{d}$  were restricted to  $|\text{Re } \bar{d}| < 0.25$ ,  $|\text{Im } \bar{d}| < 0.25$ , while the values of  $\bar{c}$  were set free.

In the most general fit (with  $P' < 0$ ), we assumed  $\epsilon = 0$  and simultaneously treated all three FSI parameters ( $\text{Re } \bar{d}$ ,  $\text{Im } \bar{d}$ ,  $\bar{c}$ ) as free. In Fig.5a we show the contour plot of the minimum of  $f$  treated as a function of complex  $\bar{d}$ . The fitted values of  $\bar{c}$  are not shown but in the region around  $\text{Re } \bar{d} = -0.22$ ,  $\text{Im } \bar{d} = +0.21$  (point X) they turn out to be close to 0. Thus, allowing  $\bar{c}$  to be free does not lead far away from the minimum found before for the  $\bar{c} = 0$  case. The corresponding  $\chi_{red}^2$  is around 1.0. The fitted values of  $|\bar{c}|$  turn out to be smaller than 0.25 for all of  $\bar{d}$  in Fig.5a with the exception of a thin slice on the right (for  $\text{Re } \bar{d} > 0.20$  and  $\text{Im } \bar{d} < 0.05$ ).

In order to show what happens for other negative as well as for positive  $\text{Re } \bar{d}$ , below we present also fits performed at two additional points ( $p1$ ) and ( $p2$ ):

$$\begin{aligned}
\text{point } p1 : \quad & \text{Re } \bar{d} = -0.10 \\
& \text{Im } \bar{d} = +0.15
\end{aligned} \tag{27}$$

and

$$\begin{aligned}
\text{point } p2 : \quad & \text{Re } \bar{d} = +0.15 \\
& \text{Im } \bar{d} = +0.15
\end{aligned} \tag{28}$$

The  $B \rightarrow PP$  branching ratios corresponding to the four cases ( $\bar{d} = 0$ ,  $\bar{c} = 0$ , point (p1), point (p2)) are gathered in Table 3 together with other fit details.

As can be seen from Table 3, the quality of the description of branching ratios at points (p1), (p2) is essentially the same as that at minimum (point  $X$ ,  $\bar{c} \approx 0$ ). Table 3 shows also that the dominant contribution to  $f$  comes from the  $2\sigma$  discrepancy between the experimental and the fitted  $B_d^0 \rightarrow \pi^0 K^0$  branching ratios (a similar problem with this decay channel can be observed in other papers, see eg. [33]). In a recent paper [39], the question of a potential discrepancy in the sum rule relating the branching ratios in  $B^+, B_d^0 \rightarrow K\pi$  decays was discussed and it was suggested that the experiment hints at a slight enhancement of both modes involving  $\pi^0$ . In our fits (as in [33]), however, the measured branching ratio of  $B^+ \rightarrow \pi^0 K^+$  is well described.

Fig.5b gives the contour plot of the corresponding fitted values of  $\gamma$ . In the region around points  $X$  and  $p1$  the fitted values of  $\gamma$  seem to be in agreement with the conservative SM expectation of  $50^\circ < \gamma_{SM} < 80^\circ$ , so this part of the complex  $\bar{d}$  plane may be called the "SM" region.

### 5.3 CP asymmetries

With the values of the FSI (and other) parameters fixed, one can attempt the calculation of CP-violating observables. The CP-violating asymmetries in  $B \rightarrow K\pi$  decays defined as

$$A_{CP}(B \rightarrow K\pi) = \frac{\Gamma(\bar{B} \rightarrow \bar{K}\pi) - \Gamma(B \rightarrow K\pi)}{\Gamma(\bar{B} \rightarrow \bar{K}\pi) + \Gamma(B \rightarrow K\pi)} \tag{29}$$

( $B = B_d^0, B^+, \bar{B} = \bar{B}_d^0, B^-$ ) were calculated for all four cases under discussion. The relevant predictions are given in Table 4 together with the experimental data ([31, 40, 41, 42, 43, 44, 45]) as averaged in [46]. The "SM" region of small  $\bar{c}$  and

negative  $\text{Re } \bar{d}$  (represented by points  $X$  ( $\bar{c} = 0$ ) and  $p1$  ( $\bar{c} = -0.11$ )) seems to describe the experimental  $B \rightarrow K\pi$  CP asymmetries somewhat better than the  $\bar{d} = 0$  case or the region of positive  $\text{Re } \bar{d}$  (ie. point  $p2$ ) do: our FSI approach prefers negative  $B^0 \rightarrow \pi^- K^+$  asymmetry, in agreement with the experiment and in disagreement with the predictions of ref.[1]. Although the  $B \rightarrow K\pi$  asymmetries are experimentally small, they might provide important model tests (see eg. [11]).

In view of the recent BaBar measurement [47] favouring a large negative asymmetry in  $B^+ \rightarrow \pi^+ \eta$  decays, we have computed the asymmetries in all  $B^+ \rightarrow \pi^+ \eta(\eta')$  and  $B^+ \rightarrow K^+ \eta(\eta')$  decays. The results are given in Table 5 with the data [47, 48, 49] averaged as in [46]. Contrary to the BaBar result, our  $B^+ \rightarrow \pi^+ \eta$  asymmetry is small and positive for  $\gamma$  in the "SM" region. On the other hand, our  $K^+ \eta$  asymmetry (fairly large when compared with other asymmetries) seems to agree with the data. Problems with the simultaneous description of  $\pi^+ \eta$  and  $K^+ \eta$  asymmetries have been noted in [46] as well.

We have also calculated parameters relevant for the time-dependent rates in  $B_d^0(t) \rightarrow \pi^+ \pi^-$  [50], ie.:

$$S_{\pi\pi} = \frac{2 \text{Im}\lambda_{\pi\pi}}{1 + |\lambda_{\pi\pi}|^2} \quad (30)$$

and

$$C_{\pi\pi} = \frac{1 - |\lambda_{\pi\pi}|^2}{1 + |\lambda_{\pi\pi}|^2}, \quad (31)$$

where

$$\lambda_{\pi\pi} \equiv e^{-2i\beta} \frac{A(\bar{B}_d^0 \rightarrow \pi^+ \pi^-)}{A(B_d^0 \rightarrow \pi^+ \pi^-)}. \quad (32)$$

Our predictions are given in Table 6. Although the experimental results from Belle and BaBar [51, 52] still exhibit the well-known discrepancies [53, 54], the "SM" region of small (negative)  $\bar{c}$  and negative  $\text{Re } \bar{d}$  (with the value of  $\gamma$  close to the SM expectations) seems favoured again.

For the time-dependent rates in  $B_d^0(t) \rightarrow \eta' K_S$ , the effect of final-state interactions is negligible. Indeed, the relevant amplitudes are dominated by the  $\bar{P}'$  and  $\bar{S}'$  amplitudes (in particular, the FSI correction is dominated by terms proportional to  $\bar{P}'$ , see Table 2). Thus, all important terms have the same weak phase. Consequently, one obtains  $S_{\eta' K_S} \approx \sin 2\beta$ ,  $C_{\eta' K_S} \approx 0$ , in agreement with the experimental averages (from [46]) of  $S_{\eta' K_S} = +0.33 \pm 0.25$ ,  $C_{\eta' K_S} = -0.18 \pm 0.16$ .

The  $B^+ \rightarrow \pi^+ \pi^0$  asymmetry is predicted to be zero (cf. Tables 1 and 2), in agreement with its experimental value of  $-0.07 \pm 0.14$  (average from [46]).

Although apart from the discrepancy in sign with the most recent BaBar  $\pi^+ \eta$

result there seems to be a hint of agreement with other asymmetries, one has to remember that these (and other) predictions for asymmetries may be affected by the inclusion of the charming penguin contribution [23, 34].

## 6 Conclusions

In this paper we have analysed the contributions from both elastic and inelastic SU(3)-breaking final-state interactions in  $B$  decays to two light pseudoscalar mesons ( $B \rightarrow PP$ ).

We have found that the inclusion of an experimentally determined pattern of SU(3) breaking in Pomeron-induced rescattering enhances the value of the  $S'/P'$  ratio when extracting it from the fit to the  $B \rightarrow PP$  branching ratios. However, taking this rescattering into account does not lead to any significant change in the overall fit. Since at the energy of  $s = m_B^2$  the inclusion of non-Pomeron elastic rescattering may lead to small corrections only, analyses incorporating full elastic FSIs can lead neither to a significant improvement in the quality of data description, nor to the extracted value of  $\gamma$  being substantially shifted towards the SM expectation.

We have pointed out that a small value of the  $B \rightarrow K^+K^-$  branching ratio *does not imply* negligible inelastic rescattering effects in other  $B \rightarrow PP$  decays. This conclusion follows from the fact that rescattering in the  $B \rightarrow K^+K^-$  decay is independent of two of the three parameters describing the totality of inelastic FSIs: one related to the  $u$ -loop long-distance penguin (in a resonance channel), and the other one describing quark rearrangement (in an exotic channel). As for  $B^+ \rightarrow K^+\bar{K}^0$ , with U-spin symmetry probably broken by final-state interactions, this decay was argued to be less helpful in the determination of the size of rescattering effects than originally suspected. Its importance in the determination of the size of rescattering effects (ie. the size of the  $u$ -loop long-distance penguin) would then lie not just in its relation to  $B^+ \rightarrow \pi^+K^0$ , but, more properly, in its relation to all other  $B \rightarrow PP$  decay channels.

Finally, after neglecting the relative strong phases of short-distance amplitudes, we have carried out fits to the available  $B \rightarrow PP$  branching ratios with all elastic and inelastic SU(3)-breaking rescattering effects taken into account. The only neglected but potentially important corrections were those due to the intermediate states composed of charmed mesons. Our fits show the importance of rescattering effects and weakly hint at the value of  $\gamma$  compatible with SM expectations. However, other

values of  $\gamma$  are also possible. Narrowing the range of admitted values of  $\gamma$  will require taking into account the experimental data on asymmetries in addition to those on branching ratios. In this paper we used the values of rescattering parameters as determined from the fits to the branching ratios, and predicted several CP-violating observables (CP asymmetries in  $B \rightarrow K\pi$  decays,  $S_{\pi\pi}$  and  $C_{\pi\pi}$  for the  $B_d^0(t) \rightarrow \pi^+\pi^-$  time-dependent decay rates etc.). Again, weak agreement with the data (with the notable exception of the  $B^+ \rightarrow \pi^+\eta$  asymmetry) was found for  $\gamma$  close to the SM expectations.

This work was supported in part by the Polish State Committee for Scientific Research (KBN) as a research project in years 2003-2006 (grant 2 P03B 046 25).

## References

- [1] M. Beneke, G. Buchalla, M. Neubert, and C. T. Sachrajda, Nucl. Phys. B606, 245 (2001)
- [2] Y. Y. Keum, H-N. Li and A. I. Sanda, Phys. Rev. D63, 054008 (2001).
- [3] L. Wolfenstein, Phys. Rev. D43, 151 (1991); M. Suzuki and L. Wolfenstein, Phys. Rev. D60,074019 (1999).
- [4] J. F. Donoghue, E. Golowich, A. A. Petrov, and J. M. Soares, Phys. Rev. Lett. 77, 2178 (1996); P. Żenczykowski, Acta Phys. Pol. B28, 1605 (1997); M. Neubert, Phys. Lett. B424, 152 (1998).
- [5] W.S. Hou, K.C. Yang, Phys. Rev. Lett. 84, 4806 (2000).
- [6] P. Żenczykowski, Phys. Rev. D63, 014016 (2001); Acta Phys. Pol. B32, 1847 (2001).
- [7] J.-M. Gerard, J. Weyers, Eur. Phys. J. C7, 1 (1999); D. Atwood, A. Soni, Phys. Rev. D58, 036005 (1998); A. Falk, A. Kagan, Y. Nir, and A. Petrov, Phys. Rev. D57, 4290 (1998).
- [8] P. Łach, P. Żenczykowski, Phys. Rev. D66, 054011 (2002).
- [9] M. Gronau, O. F. Hernandez, D. London, and J. L. Rosner, Phys. Rev. D52, 6374 (1995).
- [10] P. Żenczykowski, Acta Phys. Pol. B33, 1833 (2002).

- [11] J.-M. Gerard and C. Smith, Eur. Phys. J. C30, 69 (2003).
- [12] C. W. Chiang, J. L. Rosner, Phys.Rev.D65, 074035 (2002).
- [13] Y. Nir, Nucl. Phys. Proc. Suppl. 117, 111 (2003).
- [14] G. Buchalla, A. J. Buras, M. E. Lautenbacher, Rev. Mod. Phys. 68, 1125 (1996).
- [15] M. Neubert, J. L. Rosner, Phys. Lett. B441 (1998) 403.
- [16] A. S. Dighe, M. Gronau, and J. L. Rosner, Phys. Rev. Lett. 79, 4333 (1997).
- [17] K. M. Watson, Phys. Rev. 88, 1163 (1952).
- [18] P. Lach, Acta Phys. Pol. B34, 2631 (2003).
- [19] H. J. Lipkin, Phys. Rev. Lett. 46, 1307 (1981), Phys. Lett. B254, 247 (1991).
- [20] L. L. Chau, H.-Y. Cheng, W. K. Sze, Herng Yao, and Benjamin Tseng, Phys. Rev. D 43, 2176 (1991).
- [21] M. Gronau, J. L. Rosner, Phys. Rev. D53, 2516 (1996).
- [22] M. Beneke, and M. Neubert, Nucl. Phys. B651, 225 (2003).
- [23] M. Ciuchini, E. Franco, G. Martinelli, and L. Silvestrini, Nucl. Phys. B 501, 271 (1997); M. Ciuchini, R. Contino, E. Franco, G. Martinelli, and L. Silvestrini, Nucl. Phys. B512, 3 (1998); M. Ciuchini, E. Franco, G. Martinelli, M. Pierini, and L. Silvestrini, Phys. Lett. B515, 33 (2001).
- [24] A. J. Buras, L. Silvestrini, Nucl. Phys. B569, 3 (2000).
- [25] C. Isola, M. Ladisa, G. Nardulli, T. N. Pham, and P. Santorelli, Phys. Rev. D64, 014029 (2001); *ibid.* D65, 094005 (2002).
- [26] J. L. Rosner, Phys. Rev. D64, 094002 (2001).
- [27] P. Żenczykowski, Phys. Lett. B460, 390 (1999).
- [28] X.-G. He et al., Phys. Rev. D64, 034002 (2001).
- [29] R. Fleischer, Eur. Phys. J. C6, 451 (1999); Phys. Lett. B435, 221 (1998).
- [30] PDG Collaboration: K. Hagiwara et al., Phys. Rev. D66, 010001 (2002).
- [31] M. Yamauchi, Nucl. Phys. Proc. Suppl. 117, 83 (2003); Y. Karyotakis, Nucl. Phys. Proc. Suppl. 117, 98 (2003).

- [32] A. Höcker, H. Lacker, S. Laplace, and F. Le Diberder, Eur. Phys. J. C21, 225 (2001).
- [33] C. K. Chua, W. S. Hou, and K. C. Yang, Mod. Phys. Lett. A18, 1763 (2003).
- [34] M. Battaglia et al., "The CKM Matrix and the Unitarity Triangle", hep-ph/0304132.
- [35] J. Matias, R. Fleischer, Phys. Rev. D66, 054009 (2002).
- [36] R. Fleischer, Phys. Rep. 370, 537 (2002); R. Fleischer, "B Physics and CP Violation", hep-ph/0210323.
- [37] A. J. Buras, F. Parodi, and A. Stocchi, JHEP 0301, 029 (2003).
- [38] M. Ciuchini, G. D'Agostini, E. Franco, V. Lubicz, G. Martinelli, F. Parodi, P. Roudeau, and A. Stocchi, JHEP 0107, 013 (2001).
- [39] M. Gronau, J. Rosner, hep-ph/0307095.
- [40] CLEO Collaboration: D. Cronin-Hennessy et al., Phys. Rev. Lett. 85, 515 (2000); S. Chen et al., Phys. Rev. Lett. 85, 525 (2000); D. M. Asner et al., Phys. Rev. D65, 031103 (2002).
- [41] Belle Collaboration: B. C. K. Casey et al., Phys. Rev. D66, 092002 (2002).
- [42] BaBar Collaboration: B. Aubert *et al.*, hep-ex/0206053, presented at "Flavor Physics and CP Violation (FPCP)", Philadelphia, USA, 16-18 May 2002; Phys. Rev. Lett. 89, 281802 (2002); hep-ex/0207065, contributed to "31st International Conference on High Energy Physics (ICHEP2002)", Amsterdam, The Netherlands, July 24-31, 2002.
- [43] T. Tomura, hep-ex/0305036, presented at XXXVIII Rencontres de Moriond on Electroweak Interactions and Unified Theories, March 15-22, 2003, Les Arcs, France.
- [44] Belle Collaboration: Y. Unno et al., Phys. Rev. D68, 011103 (2003).
- [45] BaBar Collaboration: B. Aubert et al., Phys. Rev. Lett. 91, 021801 (2003).
- [46] C.-W. Chiang, M. Gronau, and J. L. Rosner, hep-ph/0306021.
- [47] BaBar Collaboration: B. Aubert *et al.*, hep-ex/0303039, presented at XXXVIII Rencontres de Moriond on QCD and High Energy Hadronic Interactions, March 22-29, 2003, Les Arcs, France.

- [48] BaBar Collaboration: B. Aubert et al., hep-ex/0303046.
- [49] Belle Collaboration: K. F. Chen et al., Phys. Lett. B546, 196 (2002).
- [50] M. Gronau, Phys. Rev. Lett. 63, 1451 (1989); M. Gronau, J. L. Rosner, Phys. Rev. D65, 09312 (2002).
- [51] BaBar Collaboration: B. Aubert et al., Phys. Rev. Lett. 89, 281802 (2002).
- [52] Belle Collaboration: K. Abe et al., Phys. Rev. D68, 012001 (2003).
- [53] T. Nakadaira, "CP violation in  $B^0 \rightarrow \pi^+\pi^-$  decay" hep-ex/0305033.
- [54] G. Hamel de Monchenault, "CP violation: recent results from BaBar" hep-ex/0305055.



## FIGURE CAPTIONS

Fig. 1. Types of rescattering diagrams: (u) uncrossed, (c) crossed.

Fig. 2. Dependence of minimized function  $f$  (Eq.(24)) on  $\gamma$ : thin lines -  $P' > 0$ , thick lines -  $P' < 0$ ; solid lines - no FSI/SU(3) symmetric Pomeron-induced FSI, dashed lines - SU(3)-breaking Pomeron-induced FSI.

Fig. 3. Dependence of minimized function  $f$  (Eq.(24)) on  $\gamma$  for full FSI: (a)  $P' > 0$ , (b)  $P' < 0$ ; solid lines -  $\bar{d} = 0$ , unrestricted  $|\bar{c}|$ ; dashed lines -  $\bar{c} = 0$ ,  $|\text{Re } \bar{d}| < 0.25$ ,  $|\text{Im } \bar{d}| < 0.25$ .

Fig. 4. Dependence of minimized function  $f$  on  $\epsilon$  for full FSI and different values of  $\gamma$ : (a)  $\bar{d} = 0$ , unrestricted  $|\bar{c}|$ ; (b)  $\bar{c} = 0$ ,  $|\text{Re } \bar{d}| < 0.25$ ,  $|\text{Im } \bar{d}| < 0.25$ .

Fig. 5. (a) Contour plot of minimized function  $f$  in complex  $\bar{d}$  plane. Positions of the minimum ( $X$ ) and of the selected points  $p1$ ,  $p2$  are indicated. (b) Contour plot of fitted values of  $\gamma$  in complex  $\bar{d}$  plane.

Table 3: Branching ratios of B decays (in units of  $10^{-6}$ )

decay	expt	$P' < 0$					
		no FSI	Pomeron	$\bar{d} = 0$	$\bar{c} = 0$	p1	p2
$B^+ \rightarrow \pi^+ \pi^0$	$5.8 \pm 1.0$	4.85	4.79	5.23	5.38	5.54	5.86
$K^+ \bar{K}^0$	$0.0 \pm 2.0$	0.57	0.51	0.54	1.09	1.02	0.87
$\pi^+ \eta$	$2.9 \pm 1.1$	2.13	2.13	3.47	2.90	2.60	2.50
$\pi^+ \eta'$	$0.0 \pm 7.0$	1.06	1.03	1.69	1.39	1.25	1.22
$B_d^0 \rightarrow \pi^+ \pi^-$	$4.7 \pm 0.5$	4.93	4.93	5.19	4.77	4.79	4.62
$\pi^0 \pi^0$	$1.9 \pm 0.7$	0.55	0.56	1.98	1.85	0.82	1.31
$K^+ K^-$	$0.0 \pm 0.6$	0	0	0	0	0	0
$K^0 \bar{K}^0$	$0.0 \pm 4.1$	0.53	0.48	0.50	1.02	0.95	0.87
$B^+ \rightarrow \pi^+ K^0$	$18.1 \pm 1.7$	18.28	18.51	19.70	19.15	18.98	20.53
$\pi^0 K^+$	$12.7 \pm 1.2$	12.96	12.87	12.47	12.15	12.34	12.76
$\eta K^+$	$4.1 \pm 1.1$	2.45	3.05	3.64	4.18	4.07	4.24
$\eta' K^+$	$75.0 \pm 7.0$	72.85	72.09	69.31	69.07	69.53	69.60
$B_d^0 \rightarrow \pi^- K^+$	$18.5 \pm 1.0$	18.90	18.90	17.57	18.89	18.99	18.10
$\pi^0 K^0$	$10.2 \pm 1.5$	6.38	6.53	6.79	7.16	7.04	7.37
$\eta K^0$	$0.0 \pm 9.3$	1.83	2.43	4.28	2.50	2.29	5.36
$\eta' K^0$	$56.0 \pm 9.0$	67.07	66.62	65.68	66.51	65.37	65.06
$f_{min}$		16.05	14.25	8.84	7.61	9.70	8.86
$ \bar{T} $		2.58	2.56	2.41	2.71	2.69	2.66
$\bar{P}'$		-4.14	-4.24	-4.34	-6.17	-5.98	-5.53
$\bar{S}'$		-1.77	-2.27	-2.09	-1.53	-1.41	-1.52
$\gamma_{fit}$		$103^\circ$	$101^\circ$	$89^\circ$	$57^\circ$	$78^\circ$	$99^\circ$
$\bar{c}$				+0.24	0	-0.11	+0.18
Re $\bar{d}$				0	-0.22	-0.10	+0.15
Im $\bar{d}$				0	+0.21	+0.15	+0.15

Table 4: Asymmetries in  $B \rightarrow K\pi$  decays

decay	expt	$P' < 0$			
		$\bar{d} = 0$	$\bar{c} = 0$	p1	p2
$B^+ \rightarrow \pi^+ K^0$	$-0.032 \pm 0.066$	0	+0.09	+0.05	-0.07
$B^+ \rightarrow \pi^0 K^+$	$+0.035 \pm 0.071$	-0.04	-0.10	-0.03	+0.03
$B^0 \rightarrow \pi^- K^+$	$-0.088 \pm 0.040$	+0.03	-0.10	-0.07	+0.08
$B^0 \rightarrow \pi^0 K^0$	$0.03 \pm 0.37$	+0.07	+0.13	+0.04	-0.05

Table 5: Asymmetries in  $B^+ \rightarrow \pi^+ \eta(\eta')$  and  $B^+ \rightarrow K^+ \eta(\eta')$  decays

decay	expt	$P' < 0$			
		$\bar{d} = 0$	$\bar{c} = 0$	p1	p2
$B^+ \rightarrow \pi^+ \eta$	$-0.51 \pm 0.19$	0	+0.10	+0.06	-0.09
$B^+ \rightarrow \pi^+ \eta'$		0	+0.10	+0.06	-0.10
$B^+ \rightarrow K^+ \eta$	$-0.32 \pm 0.20$	+0.23	-0.39	-0.49	+0.32
$B^+ \rightarrow K^+ \eta'$	$-0.002 \pm 0.040$	-0.01	+0.01	+0.01	-0.01

Table 6: CP-violating parameters in time-dependent rates for  $B \rightarrow \pi^+ \pi^-$

parameter	experiment	$P' < 0$			
		$\bar{d} = 0$	$\bar{c} = 0$	p1	p2
$S_{\pi\pi}$	Belle				
	BaBar				
$S_{\pi\pi}$	$-1.23 \pm 0.41^{+0.08}_{-0.07}$	-0.12	-0.78	-0.23	+0.49
	$-0.40 \pm 0.22 \pm 0.33$				
$C_{\pi\pi}$	$-0.77 \pm 0.27 \pm 0.08$	-0.05	-0.21	-0.08	+0.11
	$-0.19 \pm 0.19 \pm 0.05$				

Figure 1:

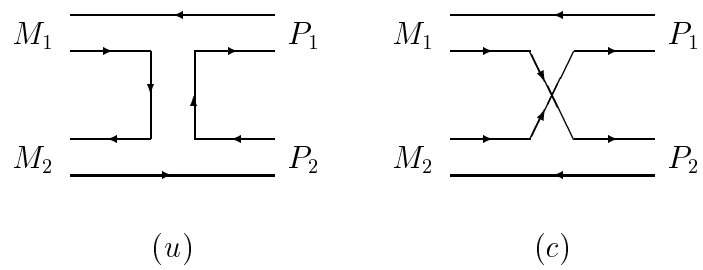


Figure 2:

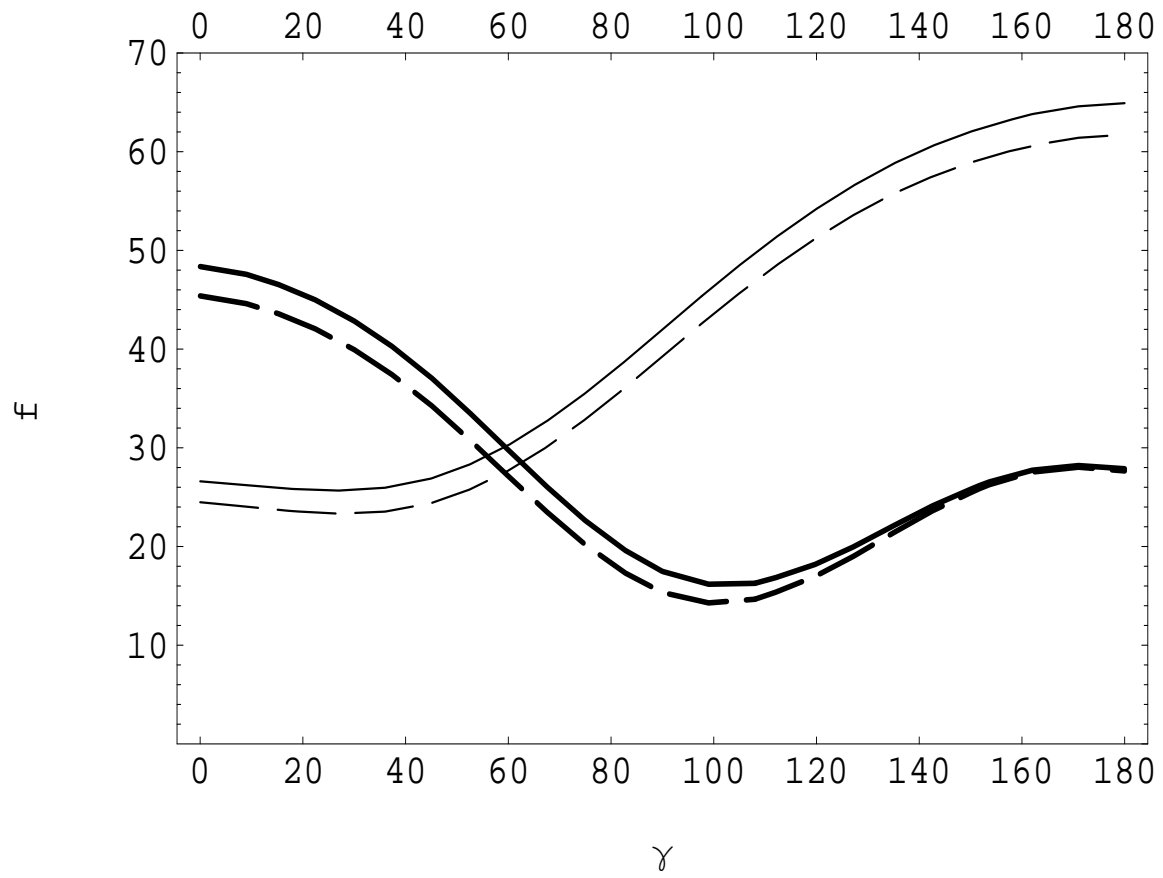
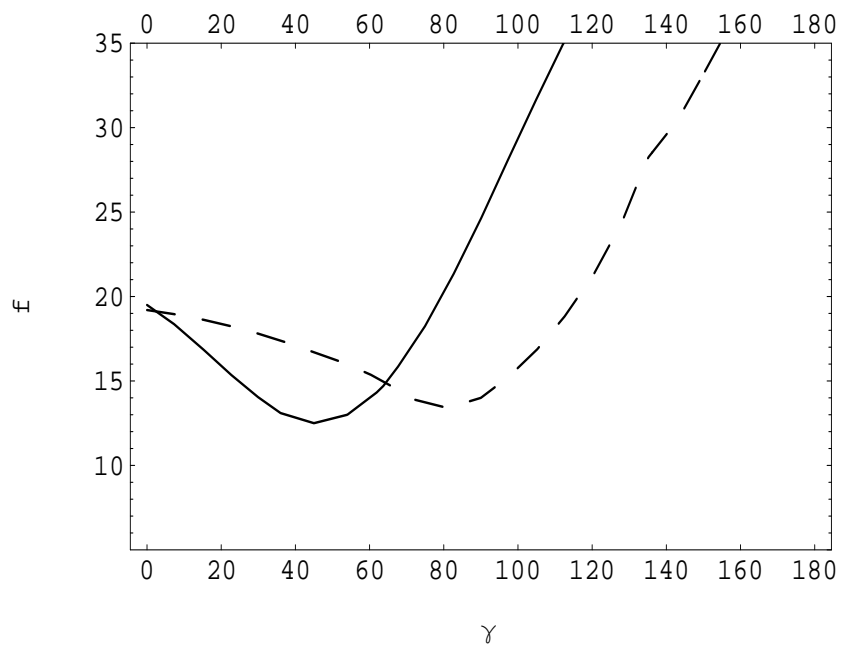


Figure 3:

(a)



(b)

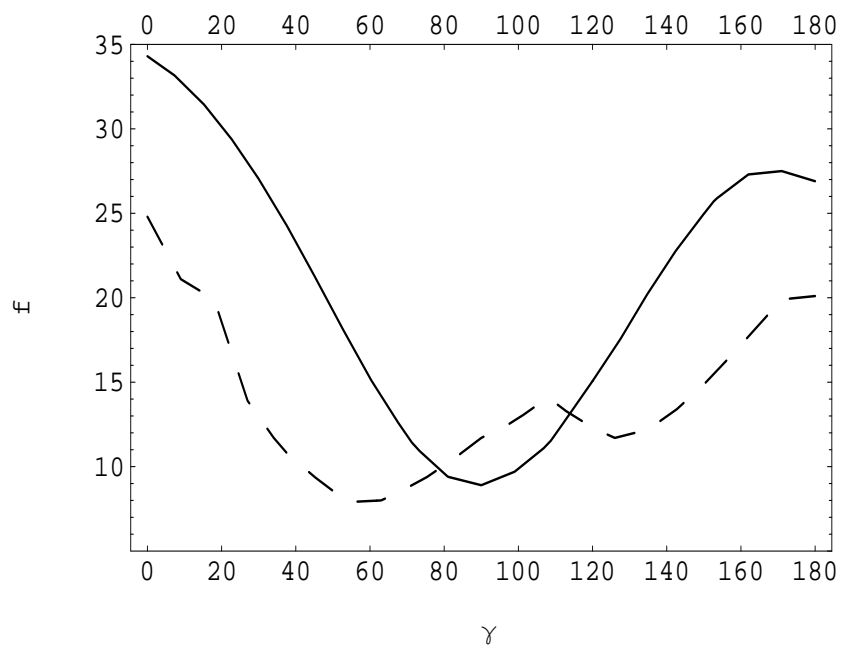
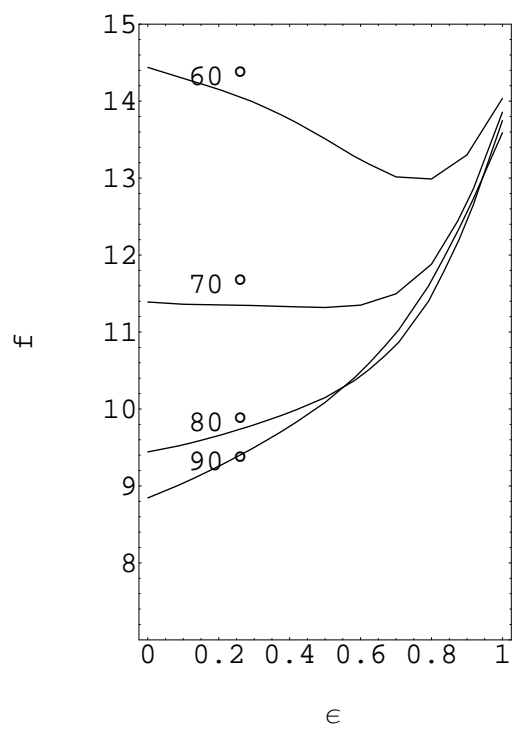


Figure 4:

(a)



(b)

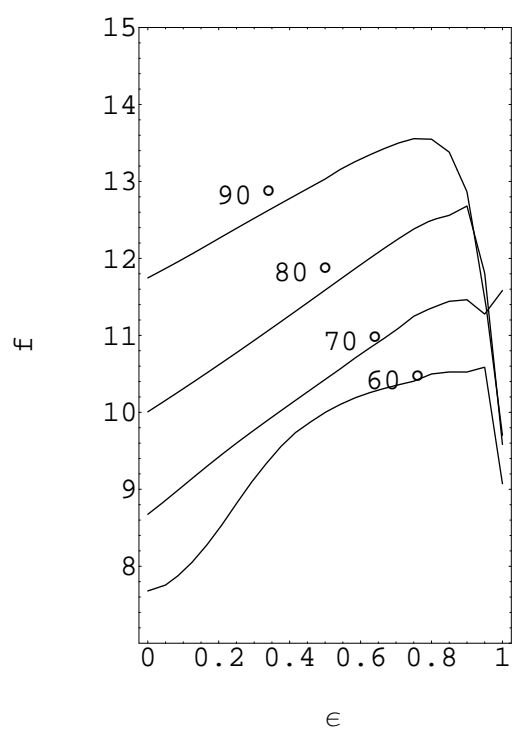
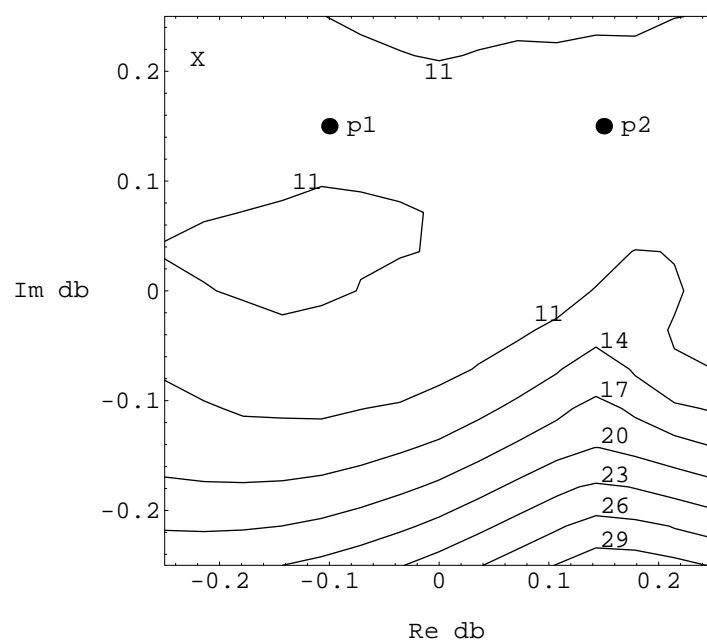


Figure 5:

(a)



(b)

